

ANISOTROPY-INDUCED WARPAGE OF A MICRO-MOLDED PART

H. J. Oh¹, Y. S. Song², D. J. Lee¹, C. G. Lee¹, J. R. Youn^{1*}

¹ Department of Materials Science and Engineering, Seoul National University, Korea

² Polymer System Division, Fiber System Engineering, Dankook University, Korea

* Corresponding author(jaeryoun@snu.ac.kr)

Keywords: *Micro-injection Molding, Liquid Crystalline Polymer (LCP), Anisotropy Properties, Reinforced Composite, Warpage, Numerical Simulation, Coefficient of Thermal Expansion (CTE)*

1 Introduction

Micro-injection molded parts required high mechanical and thermal performance, precise processability and low shrinkage have been developed in several decades. Furthermore, they are the keys of applications getting smaller. In order for a micro-injection molded part to be stable structure, it needs the high mechanical and thermal property. Also the precision of molding is the priority of a micro-structural molded product. Among polymers, liquid crystalline polymer (LCP) is one of the commonly used engineering thermoplastics satisfying the performance of a micro-molded part.

LCPs are exceptional plastics in that they maintain orientation of molecular chains of solid plastic also in melt state during injection molding process. The unique feature of thermotropic LCPs is that the molecules behave as rigid rods, this rigidity being conferred by the aromatic units and ester linkages. Therefore the mechanical and thermal applications of LCPs rely on the precise control of orientation of the rigid anisotropic molecules that form a stable liquid crystalline phase. Unlike other engineering polymers, liquid crystal polymers become significantly less anisotropic if formulated with mineral fillers or, to a lesser extent, with glass fiber reinforcement. In our recent research, this was analyzed by choosing glass fibers and minerals as the reinforcing phase and a liquid crystalline polymer as the matrix phase. Even though there are so many researches for fiber reinforced composite in isotropic matrix, few studies have addressed the complex anisotropic composite based on LCPs. A randomly oriented LCP matrix could be considered as isotropic phase but a partially or fully oriented LCP should be regarded as anisotropic phase. The anisotropic property of LCP composites can lead to

warpage of a molded part by the difference between mold shrinkage in the flow and transverse directions. In most of the researches mentioned above, the macroscopic anisotropy is measured only for a general molded part, and not much has been reported for the micro molded part. In this paper we would focus on the anisotropy of a thin molded part, especially mechanical properties and thermal expansion coefficient. In addition, warpage of micro-molded part was measured and predicted with anisotropy material properties.

2 Experimental

2.1 Materials


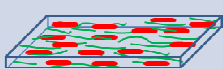

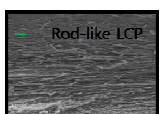

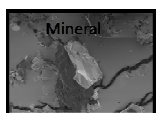
System	Fillers (wt%)		Marks
	GF	Talc	
 Single Phase : Anisotropy pure LCP matrix	-	-	S-0
 Two Phases : LCP matrix + GF	30 35	-	T-G30 T-G35
 Multi Phases : LCP matrix + GF + Talc	10 15 25	20 20 10	M-1020 M-1520 M-2510
  			

Fig.1. Summary of material systems studied in this research.

The LCP material used was Vectra A950 (Hoechst-Celanese), a commercially available, injection-grade

copolyester of about 70% p-hydroxybenzoic acid (HBA) and 30% 6-hydroxy-2-naphthoic acid (HNA). The melting temperature is reported to be 285°C. The rod shaped molecules are oriented in the flow direction during injection molding or extrusion and are rod shaped, even in the melt phase. Due to the highly ordered nature of liquid crystal polymers, mechanical properties, shrinkage and other part characteristics depend on the flow pattern in the part. In order to study the influence of fillers on the mean molecular orientation induced by injection molding, some of the experiments were performed on composites such as glass fiber reinforced composites and glass fiber and mineral reinforced hybrid composites. Both have the same chemical structure as the copolyester mentioned above, but contains, in addition, 30% and 35% by weight of chopped glass fibers, while 10%, 15% and 25% by weight of chopped glass fibers and 20%, 20% and 10% weight of minerals are included respectively. Those are summarized in figure 1.

2.2 Injection Molding

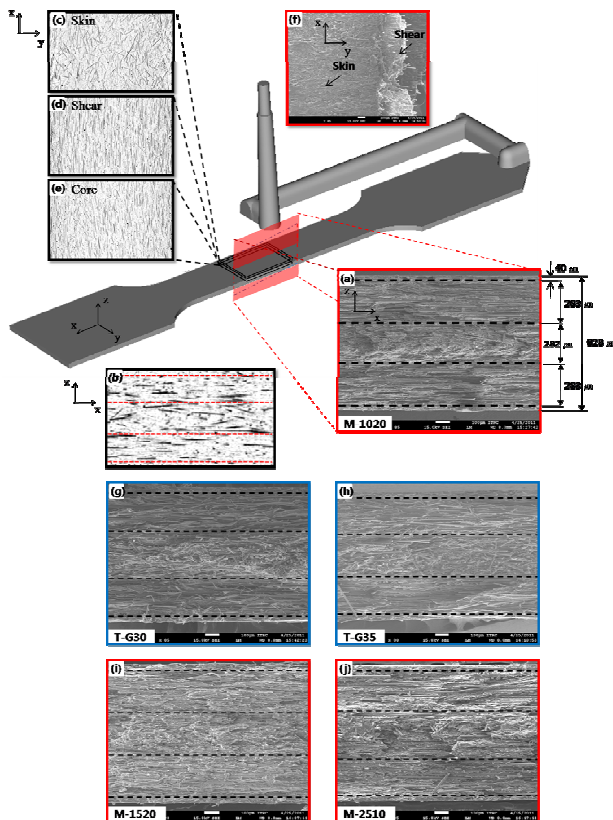


Fig.2. Flat dog-bone shaped specimens for macro-molded part: (a) and (b) the SEM image and CT

image of cross section of macro-molded part with M-1020, (c), (d) and (e) the CT images on the x-y plane at skin, shear and core plane, (f) the SEM image of the x-y plane, (g), (h), (i) and (j) the SEM images of cross section of dog-bone with T-G30, T-G35, M-1520 and M-2510.

A range of flat dog-bone shaped samples was injection molded on an industrial machine (Sumitomo SE-18DU) for macro-specimens and micro-molded parts shaped by micro-connectors also were fabricated. Figure 2 shows a picture of the dog-bone specimen, which was 150mm long and 20mm in width and the part thickness was 1mm. There are two micro-molded parts, 12mm long and 4mm in width and 250μm thick without comb-shaped pitches and with it in this study as shown in figure 3.

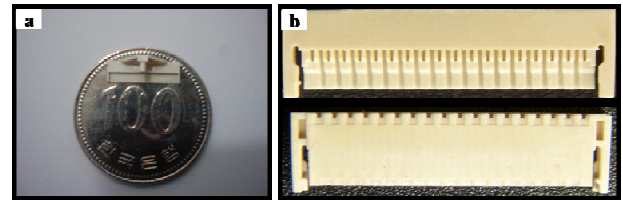


Fig.3. Micro-molded parts in this study: (a) without comb-shaped pitches and (b) with comb-shaped pitches

2.3 Observation of Orientations of Glass Fibers

A high-resolution desktop X-ray micro-tomography system (1172, Skyscan), Micro-CT, was employed to acquire micro-structural information of the talc/glass fiber reinforced composite. A 100 kV and 10 Mp X-ray source was used for the tomography to perform 2D image analysis and realistic 3D visualization with the resolution of 3μm. And image processing was implemented by using a commercial image analysis tool (Image-Pro Plus 7.0, Media Cybernetics) to acquire the information of orientation of fibers and distribution of fillers. The sections were first enhanced by controlling the contrast and brightness of the image and then transformed into binary image by thresholding method in order to discard other indistinct pixels.

2.4 Mechanical Properties

Two kinds of mechanical test were performed for measuring the elastic modulus of specimens. One of them is a tensile test performed at room temperature

according to ASTM D638. The machine utilized for the test was universal testing machine (UTM, DEC-MD 5000, DA-WHATM, Korea). The test was carried out five times for each specimen and averaged over values for the elastic modulus in the longitudinal direction. The other test was the dynamic mechanical thermal analysis (DMTA) machine (TA instrument, Q800) equipping a 3-point bending clamp used to determine the flexural modulus according to ASTM D 790. LCP specimens were fabricated as rectangular shape (45mm x 10mm x 1mm) for the test within the longitudinal direction. Also the elastic modulus in transverse direction was measured by DMTA equipped with a film tension clamp with samples (10mm x 5mm x 0.2mm).

2.5 Thermo-mechanical Properties: Coefficients of Thermal Expansion

One of factors remarkably influenced on the warpage of a micro-molded part is the coefficient of thermal expansion (CTE). It was measured by the thermal mechanical analysis (TMA) machine (Shizumadzu, TMA 60) with the film samples having rectangular shape (10mm x 5mm x 0.2mm) in which molecules and glass fibers were oriented in the flow direction, respectively. Increasing heat rate and range of temperature were 5°C/min and room temperature to 175°C. The test was examined in N2 atmosphere.

2.6 SEM Observation

The SEM(Scanning Electron Microscope) study was carried out with a SUPRA 55VP (Carl Zeiss, Germany) with 100~50,000 times magnification. Fractured surface of the each specimens was coated by Sputter coater: (BAL-TEC/SCD 005)

2.7 X-ray Diffraction

Rectangular samples of approximately 10 x 5 mm were cut from the each layer of the injection-molded specimens, as shown in figure 2(c), (d) and (e). A Bruker D5005 Power X-ray Diffractometry was used for the x-ray analysis. A CuK α X-ray tube with a long fine focus was used with a power setting of 40 kV and 30 mA. The divergence slit and the scatter slit were fixed at 1°, with the receiving slit

having an opening of 0.1 mm. The scan used was at 0.02° per step, with 1 s allowed for each step, yielding 50 s per degree of 2 θ . This range is sufficient to cover all the major crystalline peaks for LCP.

3 Numerical Calculation

3.1 Fiber Orientation Distribution

When melting polymer is injected into a cavity, reinforcements are also flowing into the cavity being oriented in accordance with velocity gradient, cavity geometry, packing pressure, etc. Xia et al. [17] proposed a two-parameter exponential function in their work to model a fiber orientation distribution in the injection molded specimens. The fiber orientation distribution function is as follows:

$$g(\theta) = \frac{(\sin \theta)^{2p-1} (\cos \theta)^{2q-1}}{\int_{\theta_{\min}}^{\theta_{\max}} (\sin \theta)^{2p-1} (\cos \theta)^{2q-1} d\theta} \left(0 \leq \theta \leq \frac{\pi}{2} \right) \quad (1)$$

$$\theta_{\text{mod}} = \arctan \left\{ \frac{2p-1}{\sqrt{2q-1}} \right\} \quad (2)$$

where p and q are shape parameters and θ_{mod} is a most probable fiber orientation angle derived by differentiating the fiber orientation distribution function.

To characterize the fiber orientation of the composite, Fakirov and Fakirova proposed the orientation factor as defined below:

$$f_p = 2 \langle \cos^2 \theta \rangle - 1 \quad (3)$$

$$\text{where } \langle \cos^2 \theta \rangle = \frac{\sum_i N(\theta_i) \cos^2 \theta_i}{\sum_i N(\theta_i)}$$

and θ_i represents an angle between the individual fibers and the primary axis, and $N(\theta_i)$ the number of fibers under certain angle θ_i . The orientation factor ranges from -1 to +1. For random planar distribution $f_p = 0$ and for perfect alignment along the principal axis, $f_p = \pm 1$.

Another theory for the quantification of the fiber orientation commonly used and well established is the fiber orientation tensor proposed by Cintra and Tucker. For continuous fiber distribution the orientation follows as below:

$$a_{ij} = \frac{\int_L \int_P P_i P_j L \psi(P, L) dP dL}{\int_L \int_P L \psi(P, L) dP dL} \quad (4)$$

When we deal with the practical composites, discrete fiber samples are measured, so the components of tensors are calculated by a summation instead of the integration:

$$a_{ij} = \frac{\sum (p_i p_j) F_n}{\sum F_n} \quad (5)$$

$$\text{where } F_n = \frac{1}{\cos \theta_n}$$

3.2 Mean-field Homogenization of Composite Materials

We consider heterogeneous materials whose microstructure consists of a matrix material, transversely isotropy LCP, and multiple phases of so-called “inclusions”, which is glass fibers or minerals.

The purpose of mean-field homogenization(MFH) is to compute approximate but accurate estimates of the volume averages of the stress and strain fields. In this study, Mori-Tanaka model was applied to calculate the CTE of composites. The derivation is based on an approximate use of Eshelby’s solution. It is found that the stiffness tensor relating the volume average of strain over all inclusions to the mean matrix strain is given by:

$$C^{M-T} = C^m \left\{ I + f \left[(1-f)(C^f - C^m)E + C^m \right]^{-1} (C^f - C^m) \right\} \quad (6)$$

The Mori-Tanaka model is very successful in predicting the effective properties of two-phase composites. Multi-phase composites are made of a matrix material and at least two inclusion phases which differ in terms of materials, aspect ratio or orientation. The multi-level method is based on nested homogenization levels. It is illustrated in figure 4 for a three-phase composite and proceeds as follows. At the deepest level, level 2 in figure 4, the real matrix material is homogenized with a first family of inclusions, the black ones in figure 4. The effective material thus obtained plays the role of a fictitious matrix, in grey in figure 4, which is reinforced with another set of inclusions, in blue in figure 4. This is an upper level which is itself homogenized, level 1 in figure 4, and so on until all inclusion families have been accounted for.

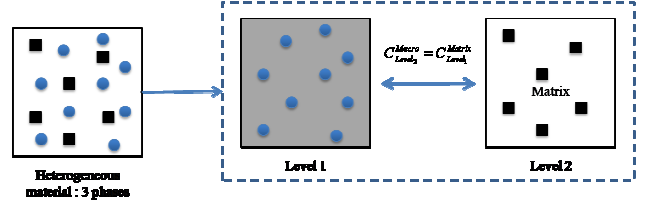


Fig.4. Multi-level method. Left : three-phase composite to be homogenized. Right : deeper level 2 : real matrix with “black” inclusions. Middle : upper level 1 the homogenized composite from level 2 plays the role of a fictitious matrix (in grey) reinforced with “blue” inclusions.

3.3 Thermal Flow Simulation

The governing equations needed for multiscale modeling of micro-cavity and macro-cavity are the conservation of mass, conservation of momentum and conservation of energy equations as follows:

$$\frac{D\rho}{Dt} + \rho(\nabla \cdot \mathbf{v}) = 0 \quad (7)$$

$$\rho \frac{D\mathbf{v}}{Dt} = \nabla \cdot \boldsymbol{\tau} - \nabla P + \rho \mathbf{g} = 0 \quad (8)$$

$$\rho C_p \frac{DT}{Dt} = \beta T \frac{DP}{Dt} + \eta \dot{\gamma}^2 + \nabla \cdot \mathbf{q} = 0 \quad (9)$$

where ρ is the density of polymer, \mathbf{v} is the velocity vector, P is the pressure, $\boldsymbol{\tau}$ is the viscous stress tensor, \mathbf{g} is the gravity vector, C_p is the specific heat at a constant pressure, β is the coefficient of thermal expansion, η is the generalized Newtonian viscosity, \mathbf{q} is the heat flux, and $\dot{\gamma}$ is the shear rate, which is defined as

$$\dot{\gamma} = \sqrt{\left(\frac{\partial u}{\partial z} \right)^2 + \left(\frac{\partial v}{\partial z} \right)^2} \quad (10)$$

Here, (u, v) indicate the velocity vector in the x and y directions. The flow front in the cavity is tracked using a fluid concentration equation expressed as follows:

$$\frac{DF}{Dt} = 0 \quad (11)$$

where F is the fluid concentration. In the current study, the LCP polymer melt was regarded as a non-Newtonian viscous fluid. Non-Newtonian viscosity can be represented using the modified Cross model.

$$\eta(T, \dot{\gamma}, p) = \frac{\eta_0(T, p)}{1 + (\eta_0(T, p) \dot{\gamma} / \tau^*)^{1-n}} \quad (12)$$

where η denotes the viscosity, η_0 is the zero shear rate viscosity, τ^* is the shear stress at the transition between the Newtonian behavior and the power law behavior, and n is the power law index. According to the Williams-Landel-Ferry (WLF) equation, η_0 can be written as a function of temperature:

$$\eta_0(T, p) = D_1 \exp\left(-\frac{A_1(T - T^*(p))}{A_2 + D_3 p + (T - T^*(p))}\right) \quad (13)$$

where $T^*(p) = D_2 + D_3 p$.

4 Results and Discussion

4.1 Orientation: Definition of Layers

In order to fabricate a successful micro-molded part, the characteristics of LCP composite material should be correctly defined with its anisotropy properties. Preferentially, the layers of an injection molded part illustrated in figure 2. The skin-shear-core morphology is in fact made up of three distinct layers within the thickness. The first layer, named 'skin layer', is created from a rapid quenching effect of the polymer flow, which is in contact with the cold mold wall. It results from the solidification from molten state, where the polymer was previously summated to intensive shear and elongational stresses. In this layer, glass fibers randomly oriented in the x-y plane. The formation of the 'skin layer' leads to two opposite effects. It both reduces the flow cross-sectional area and promotes the creation of a thermal insulating barrier for the central molten polymer, leading to respectively an increasing in the shear stresses and a decrease in the cooling rates. These effects favor the flow-induced orientation, and in particular the formation of highly oriented glass fibers. The name given to this region is 'shear layer', with an average thickness ranging from a few hundredths of a micron. The center of the flow cools slowly, allowing the relaxation of previously oriented glass fibers. The glass fibers randomly oriented within a three-dimensional volumetric layer. This layer, named 'core layer', possesses the biggest crystallinity.

4.2 Characteristics of Material Properties

LCP material might be regarded as the transversely isotropic material if molecules were oriented into one direction (flow direction). The shear layer was

proper to introduce the transversely isotropy material in this studies, even though glass fibers reinforced in it as shown figure 5 and 6.

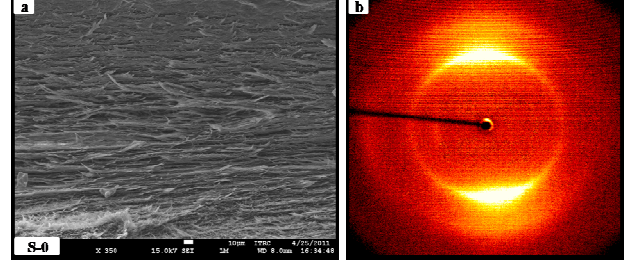


Fig.5. Shear layer of the pure LCP(S-0) : (a) SEM image of S-0 with micro fibril structure, (b) 2D WAXD pattern of the shear layer

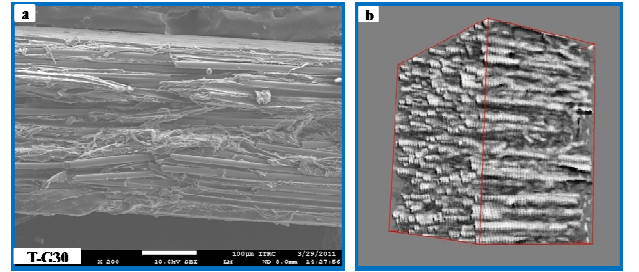


Fig.6. Shear layer of the glass fiber reinforced LCP composite(T-G30) : (a) SEM image of T-G30, (b) 3D CT scanning image

Most important material property for the warpage of micro-molded part is the CTE of a material and the micro-structure of micro-molded part. Figure 7 shows the structure of a micro-molded part distinguished from a macro-molded part. It was made up of just two layers, such as skin and core layer. The CTE of material systems measured in this study was compared with calculations by Mori-Tanaka model in figure 8.

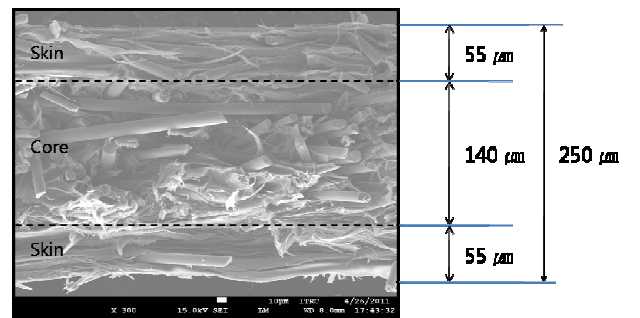


Fig.7. SEM image of micro-molded part with the glass fiber reinforced LCP composite(T-G30)

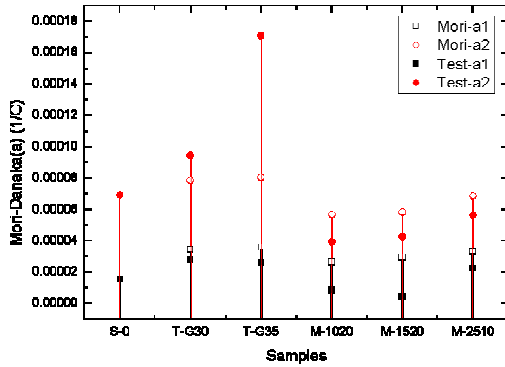


Fig.8. The measured values of CTE compared with values of calculated with Mori-Tanaka model.

4.3 Warpage of Micro-molded Parts

The micro-molded parts examined by the FEM for orientation and warpage analysis as shown in figure 9 and 10. The fiber orientation was predicted successfully compared with CT image of a micro-molded part. Furthermore, various CTE values were tested on the warpage analysis as shown in figure 10.

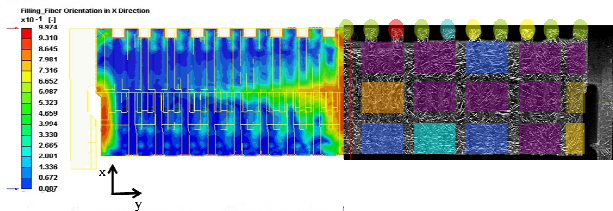


Fig.9. The glass fiber orientation tensor for a micro-molded part. Left : thermal flow simulation. Right : illustration on CT image of a practical micro-molded part.

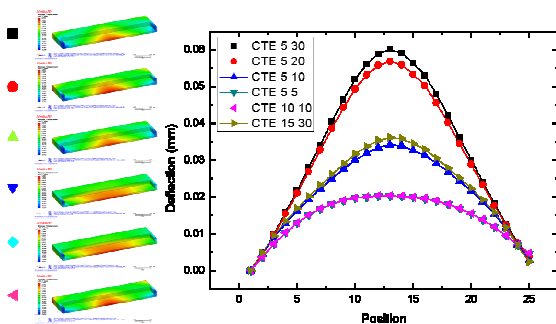


Fig.10. Warpage analysis of a micro-molded part with various CTE values.

Consequently, we considered the measured CTE values on the warpage simulation of a micro-molded part in figure 11. It was the best prediction of warpage of micro-molded part.

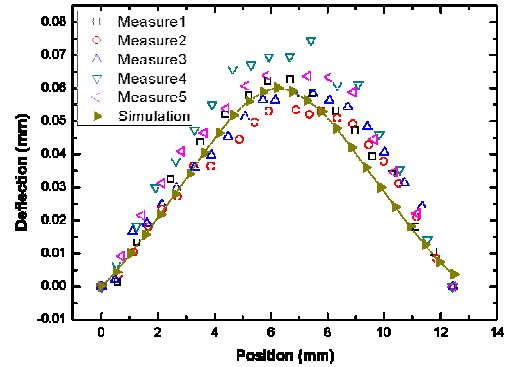


Fig.11. Warpage prediction with the measured CTE values compared with measured values of a micro-molded part.

5 Conclusions

An analytical procedure was proposed and validated for predicting the warpage of hybrid LCP composites, where fillers are glass fiber and talc. There are two specimens, injection molded, to measure the properties of the composite and to validate the warpage of a micro-molded part. The modeling strategy of the predicting the elastic moduli and thermal expansion behavior was validated by experimental with considering the orientation of fillers. The injection molded sample was tested to measure the coefficient of thermal expansion (CTE) and anisotropic moduli. The orientation of glass fibers was investigated by the computed tomography (CT) and quantified through the orientation tensor. The numerical analysis of warpage for a micro-molded part was performed with the properties obtained from experiments and prediction. In order to obtain better prediction of the orientation field for glass fibers, the fiber-fiber interaction coefficient was adjusted into a practical orientation field of the micro-molded part. The key result was that if material properties and orientation field was matched with practical one, the best prediction was obtained from the numerical prediction.